Accumulation and purging of deleterious mutations through severe bottlenecks in ibex

Christine Grossen[1,*], Frederic Guillaume[1], Lukas F. Keller[1,2,a,*], Daniel Croll[3,a,*]

[1]Department of Evolutionary Biology and Environmental Studies, University of Zurich, Zurich, Switzerland

[2]Zoological Museum, University of Zurich, Karl-Schmid-Strasse 4, Zurich, Switzerland

[3]Laboratory of Evolutionary Genetics, Institute of Biology, University of Neuchâtel, Neuchâtel, Switzerland

[a] LFK and DC contributed equally to this work

[*]Authors for correspondence: christine.grossen@ieu.uzh.ch, lukas.keller@ieu.uzh.ch, daniel.croll@unine.ch

Author contributions:

Conception and design of study: CG, DC, LFK

Acquisition and analysis of data: CG

Interpretation of data: CG, DC, LFK, FG

Funding: CG, LFK

Wrote the manuscript with input from the other authors: CG, DC

Abstract

Population bottlenecks have a profound impact on the genetic makeup of a species including levels of deleterious variation. How reduced selection efficacy and purging interact is known from theory but largely lacks empirical support. Here, we analyze patterns of genome-wide variation in 60 genomes of six ibex species and the domestic goat. Ibex species that suffered recent severe bottlenecks accumulated deleterious mutations compared to other species. Then, we take advantage of exceptionally well-characterized repeated bottlenecks during the restoration of the near-extinct Alpine ibex and show that experienced bottleneck strength correlates with elevated individual inbreeding. Strong bottlenecks led to the accumulation of mildly deleterious mutations and purging of highly deleterious mutations. We show in a simulation model that realistic bottleneck strengths can indeed simultaneously purge highly deleterious mutations during overall mutation accumulation. Genome-wide purging of highly deleterious mutation load over few generations in the wild has implications for species conservation efforts.

Main text

Dramatic, temporary reductions in population size – so-called bottlenecks – occur in nearly all plant and animal populations including humans [1]. These demographic changes have important consequences for wildlife management and the conservation of endangered species [2], but they also have profound consequences including genetic disorders [e.g 3-7]. Increased genetic drift and inbreeding due to bottlenecks lead to loss of neutral genetic variation, a reduced efficacy of natural selection, and increased expression of deleterious recessive mutations [8-10]. The expression of recessive mutations under inbreeding creates the potential for selection to act against these mutations, a process known as purging. Purging reduces the frequency of deleterious mutations depending on the population size, the degree of dominance, and the magnitude of the deleterious effects [11]. Unless population sizes are extremely low, bottlenecks tend to purge highly deleterious, recessive mutations [11,12]. On the other hand, genetic drift during bottlenecks reduces the efficacy of selection [13]. This allows mildly deleterious mutations to drift to substantially

51 higher frequencies [6,14]. The combination of purging and reduced selection efficacy generates complex
52 dynamics of deleterious mutation frequencies following population bottlenecks [11,12,15-17].
53
54 Theory predicts how reduced selection efficacy and purging impact the mutation load through
55 bottlenecks [11,15,16,18], but genetic evidence from wild populations is rare [19-21]. Most previous research
56 used changes in fitness to infer possible purging events [18,21-24], but changes in fitness can result from
57 causes unrelated to purging such as adaptation to specific environmental conditions or the fixation of
58 deleterious mutations [10,25]. One study provided direct evidence for purging of the most deleterious
59 mutations in isolated mountain gorilla populations that split off larger lowland populations ~20'000
60 years ago [19]. However, it remains unknown how more complex or recent demographic events affect
61 levels of deleterious mutations in the wild. Here, we take advantage of exceptionally well characterized
62 repeated bottlenecks during the reintroduction of the near-extinct Alpine ibex to retrace the fate of
63 deleterious mutations. Alpine ibex were reduced to ~100 individuals in the 19th century in a single
64 population in the Gran Paradiso region of Northern Italy [26]. In less than a century, a census size of ca.
65 50’000 individuals has been re-established across the Alps. Thus, the population bottleneck of Alpine
66 ibex is among the most dramatic recorded for any successfully restored species. Most extant populations
67 experienced at least three bottlenecks leaving strong footprints of low genetic diversity [27,28].
68

Figure 1

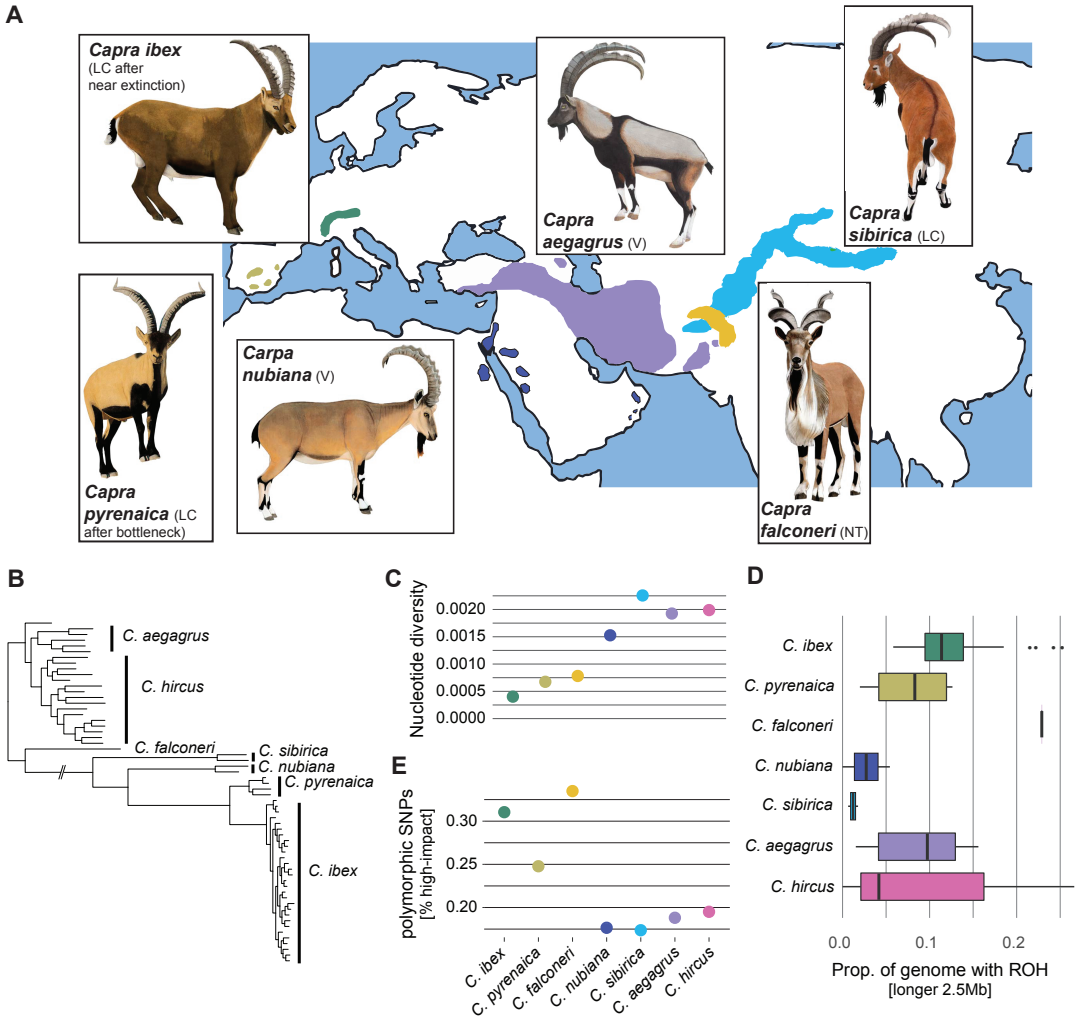

Figure 1: Characterization of sampled ibex species. A) Geographical distribution and IUCN conservation status of ibex and wild goat species (LC: Least concern, V: Vulnerable, NT: Near threatened [60]). Sample izes: *C. ibex*: N=29, *C. pyrenaica*: N=4, *C. aegagrus*: N=6, *C. sibirica*: N=2, *C. falconeri*: N=1, *C. nubiana*: N=2. B) Maximum likelihood phylogenetic analyses, C) nucleotide diversity, D) proportion of the genome with runs of homozygosity (ROH) longer than 2.5 Mb and E) percentage of polymorphic sites within species that segregate highly deleterious mutations.

We analyze 60 *Capra* genomes covering Alpine ibex (*C. ibex*), five additional wild goats and the domestic goat, we find exceptionally low genome-wide variation and an accumulation of deleterious mutations in Alpine ibex (Figure 1). Both nucleotide diversity and number of heterozygous sites per kb sequenced was lowest in Alpine ibex and Iberian ibex (*C. pyrenaica*), the two species that experienced the strongest recent bottlenecks (Figure 1C, Figure S2, Tables S1 and S2). Genome-wide diversity was highest in Siberian ibex (*C. sibirica*), which have large and relatively well-connected populations [29].

84 Genomes of the Siberian and Nubian ibex (*C. nubiana*) and of some domestic goat (*C. aegagrus hircus*)
85 showed the least evidence for recent inbreeding estimated by genome-wide runs of homozygosity
86 (ROH) [30]. In contrast, the genomes of some Alpine ibex, the Markhor (*C. falconeri*), and some domestic
87 goat individuals contained more than 20% ROH (Figure 1D, Figures S3A and B, Table S3). Overall,
88 there was clear genomic evidence that the near extinction and recovery of the Alpine ibex resulted in
89 substantial genetic drift and inbreeding, opening the possibility for purging and accumulation of
90 deleterious mutations.
91
92 We analyzed all *Capra* genomes for evidence of segregating deleterious mutations (Figure S6). We
93 restricted our analyses to autosomal coding sequences with evidence for transcriptional activity in
94 Alpine ibex organs. We further removed sites with low genomic evolutionary rate profiling (GERP) [31]
95 scores yielding a total of 370'853 SNPs (Table S4). We functionally annotated SNP variants for the
96 expected impact on the protein function. We found that across all seven *Capra* species 0.17% of these
97 SNPs carried a highly deleterious variant with the majority incurring a stop-gain mutation (Table S4).
98 We found that the proportion of highly deleterious mutations varied substantially among *Capra* species
99 (Figure 1E, Figures S7A to D). The proportion of highly deleterious variants segregating within species
100 was inversely correlated with nucleotide diversity (Pearson, df=5, r=-0.86, p=0.012). Hence, the *Capra*
101 species with the smallest populations or the most severe population size reductions show an
102 accumulation of deleterious mutations.
103
104 Both Alpine and Iberian ibex experienced severe bottlenecks due to overhunting and habitat
105 fragmentation. Historic records indicate that Alpine ibex suffered a bottleneck of ~100 individuals at
106 the end of the 19th century and Iberian ibex a bottleneck of ~1000 individuals [32] (Table S1). We first
107 looked for evidence of purging in the allele frequency spectra of mutation classes of varying severity.
108 We focused only on derived sites that were polymorphic in at least one of the two sister species (Figure
109 2A, S8). We found that frequency distributions of high and moderate impact mutations in Alpine ibex
110 were downwards shifted indicating purifying selection (Figure 2C and GERP score analyses in Figure
111 S9A). Short indels (≤ 10 bp) in coding sequences revealed a similar shift towards lower frequencies

(Figure S9B). This is consistent with stronger selection acting against highly deleterious mutations in Alpine ibex.

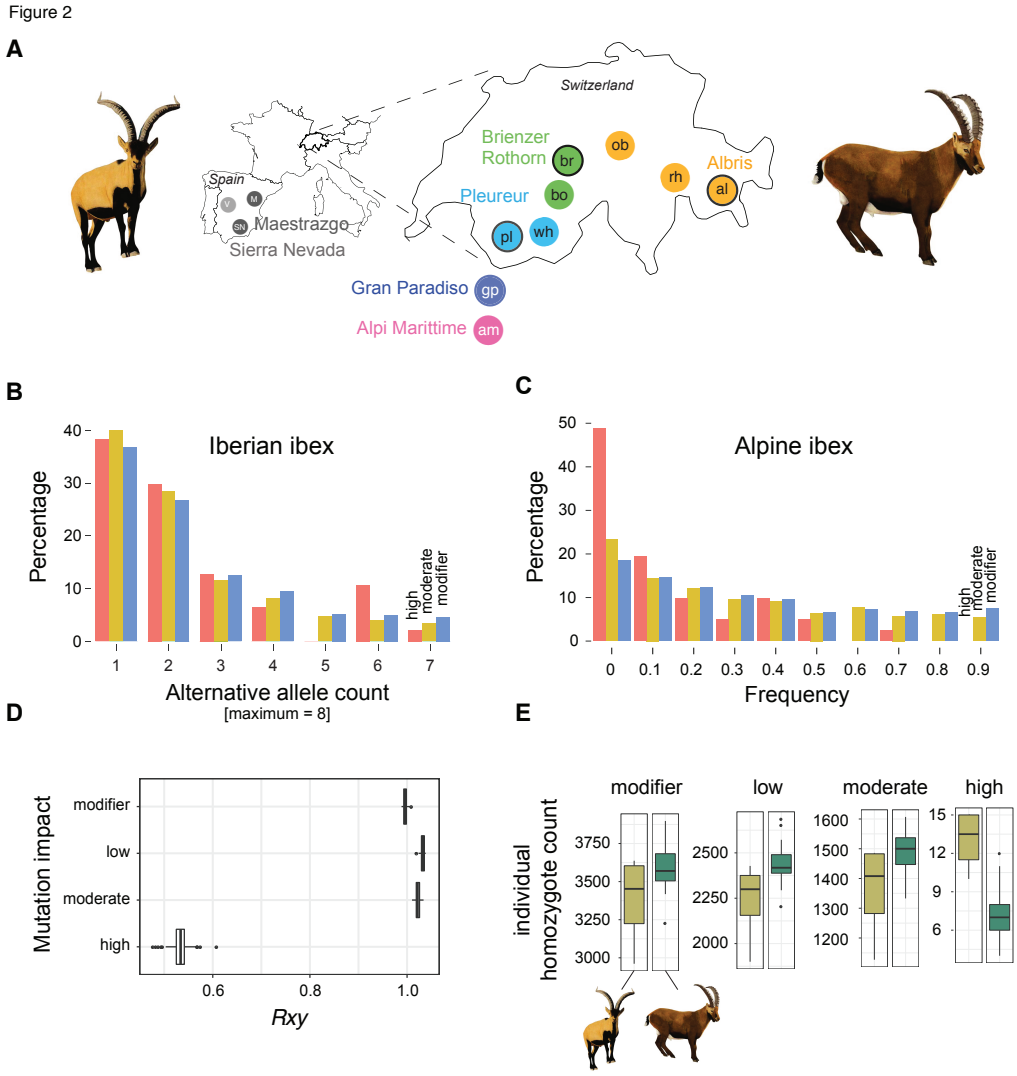

Figure 2: Segregating deleterious mutations in Alpine and Iberian ibex. A) Population sampling locations of Iberian ibex (left, grey circles) and Alpine ibex (right, colored circles). Each filled circle represents a population. Circles with a black outline indicate the first three reintroduced populations in Switzerland that were used for all subsequent population reintroductions of Alpine ibex. Colors associate founder and descendant populations (see also Figure 3A). Site frequency spectra for neutral (modifier), mildly (moderate impact) and highly deleterious (high impact) mutations for (B) Iberian and (C) Alpine ibex. D) *Rxy* analysis contrasting Iberian with Alpine ibex across the spectrum of impact categories. *Rxy* < 1 indicates a relative frequency deficit of the corresponding category in Alpine ibex compared to Iberian ibex. E) Individual homozygote counts per impact category for Iberian (light green) and Alpine ibex (dark green).

128 To test whether Alpine ibex indeed showed evidence for purging of deleterious mutations compared to
129 Iberian ibex, we calculated the relative number of derived alleles *Rxy* [33] for each mutation impact
130 category (Figure 2D). We used a random set of intergenic SNPs for standardization, which makes *Rxy*
131 robust against sampling effects and population substructure [33]. Low and moderate impact mutations (*i.e.*
132 mildly deleterious mutations) showed a minor excess in Alpine ibex compared to Iberian ibex,
133 indicating a higher load in Alpine ibex. In contrast, we found that highly deleterious mutations were
134 strongly reduced in Alpine ibex compared to Iberian ibex (Figure 2D). Strikingly, the proportion of
135 SNPs across the genome segregating a highly deleterious mutation is higher in Alpine ibex (Figure 1E),
136 but *Rxy* shows that highly deleterious mutations have a pronounced downwards allele frequency shift
137 in Alpine ibex compared to Iberian ibex (Figure 2C). Furthermore, the number of homozygous sites
138 with highly deleterious mutations per individual were considerably lower in Alpine ibex than Iberian
139 ibex (Figure 2E). Together, this shows that highly deleterious mutations were substantially purged in
140 Alpine ibex. We also found evidence for the accumulation of mildly deleterious mutations through
141 genetic drift in Alpine ibex.
142
143 Consistent with the fact that all extant Alpine ibex originate from the Gran Paradiso, this population
144 occupies the center of a principal component analysis (Figure 3A-B, Figure S11A-B; [28]). The first
145 populations re-established in the Alps were already clearly distinct from the Gran Paradiso source
146 population and showed reduced nucleotide diversity (Figure 3A, C), having experienced 1 or 2
147 additional bottlenecks [27]. These initial three reintroduced populations were used to establish additional
148 populations, which underwent a total of 3-4 bottlenecks. These additional bottlenecks lead to further
149 loss of nucleotide diversity and genetic drift, as indicated by the increasing spread in the principal
150 component analysis (Figure 3A-C). An exceptional case constitutes the Alpi Marittime population,
151 which was established through the translocation of 25 Gran Paradiso individuals of which only six
152 successfully reproduced [34]. As expected from such an extreme bottleneck, Alpi Marittime showed
153 strong genetic differentiation from all other Alpine ibex populations and highly reduced nucleotide
154 diversity (Figures 3B-C; [35]). To estimate the expected strength of drift experienced by different
155 populations, we estimated effective population sizes through the long-term harmonic mean population

sizes based on demographic records spanning the near century since establishment [36,37]. We found that both the nucleotide diversity and the individual number of heterozygous sites per kb decreased with smaller long-term population size (Figure 3C, Figure S12). In parallel to genetic drift, inbreeding was also higher in the populations with the lowest harmonic mean population sizes. Genomes from the Gran Paradiso source population generally showed the lowest proportions of the genome affected by ROH, while reintroduced populations of lowest effective population size had the highest proportions of the genome affected by ROH (Figure 3D and Figure S3).

Figure 3

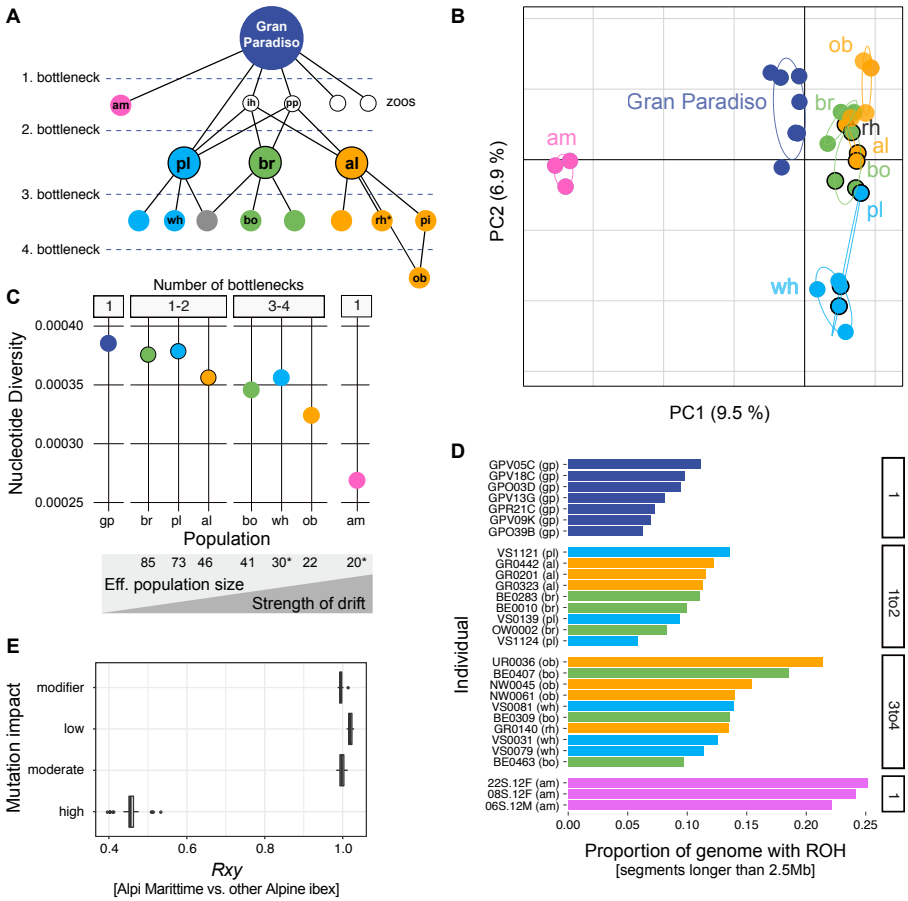

Figure 3: Population genomic consequences of Alpine ibex recolonization. A) Schematic showing the recolonization history and population pedigree of Alpine ibex. Locations include also zoos and the population Pilatus (pi), which was not sampled for this study but is known to have contributed to the population Oberbauenstock (ob). am: Alpi Marittime, gp: Gran Paradiso; ih: Zoo Interlaken Harder; al: Albris; bo: Bire Öschinen; br: Brienzer Rothorn; ob: Oberbauenstock; pl: Pleureur; rh: Rheinwald; wh: Weisshorn; pi: Pilatus; pp: Wildpark Peter and Paul. The grey circle represents a population that was founded from more than one population. Figure elements were modified from Biebach and Keller (2009) with permission. B) Principal component analysis of all Alpine ibex individuals included in the study. C) Nucleotide diversity per population. D) Proportion of the genome within runs of homozygosity (ROH) longer than 2.5 Mb. E) *Rxy* analysis contrasting the strongly bottlenecked Alpi Marittime population with all other Alpine ibex populations across the spectrum of impact categories. *Rxy* < 1 indicates a relative frequency deficit of the corresponding category in the Alpi Marittime population. Circles with a black outline indicate the first three reintroduced populations in Switzerland that were

used for all subsequent population reintroductions of Alpine ibex. Colors associate founder and descendant populations.

Bottlenecks should affect deleterious mutations by randomly increasing or decreasing allele frequencies at individual loci. As predicted from theory, we find that individuals from populations that underwent stronger bottlenecks carry significantly more homozygotes for modifier, low and moderate impact mutations (*i.e.* nearly neutral and mildly deleterious mutations; Figure 4A). In contrast, individuals showed no meaningful difference in number of homozygotes for high impact (*i.e.* highly deleterious) mutations across populations. The stability in the number of homozygotes for high impact mutations through successive bottlenecks despite a step-wise increase in the number of homozygotes for weaker impact mutations, strongly suggests that purging occurred over the course of the Alpine ibex reintroductions. This finding was confirmed using an alternative categorization of deleterious mutation load based on phylogenetic conservation based GERP scores (Figure S13). Because the above findings are contingent on a model where deleterious mutations are recessive, we also analyzed the total number of derived alleles per individual. We find a consistent but less pronounced increase in total number of derived alleles per individual for nearly neutral and mildly deleterious mutations (Figure 4B). In contrast, the total number of derived alleles for highly deleterious mutations did not correlate with the strength of bottleneck and was lowest in the most severely bottlenecked Alpi Marittime population (Figure 4B), suggesting that the most deleterious mutations were purged in this population. The *Rxy* statistics showed a corresponding strong deficit in the Alpi Marittime population (Figure 3E). This is consistent with substantially more purging in the most bottlenecked Alpine ibex population.

Figure 4

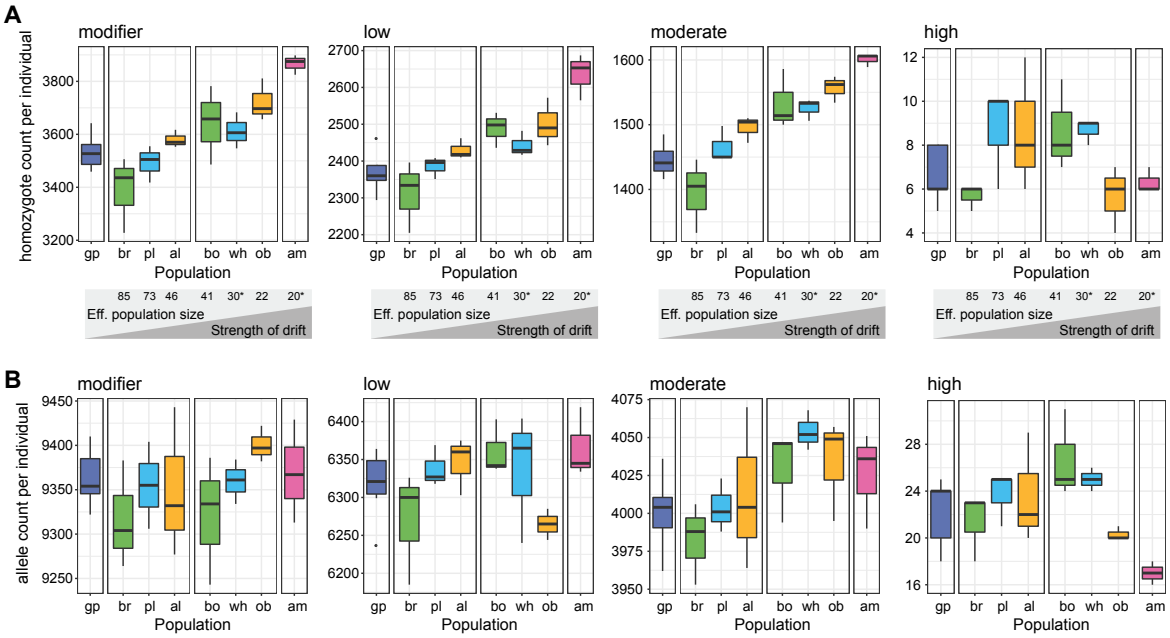

Figure 4: Impact of recolonization on the mutation load per individual. (A) Homozygote counts and (B) allele counts per individual for each Alpine ibex population. The schematic between A and B indicates the harmonic mean of the census size of each population, which is inversely correlated with the strength of drift. *) Estimated numbers. Colors associate founder and descendant populations (see also Figure 3A).

We analyzed the predicted protein truncation by highly deleterious mutations using homology-based inferences. Focusing on high-impact mutations segregating in Alpine ibex, we found that nearly all mutations disrupted conserved protein family (PFAM) domains encoded by the affected genes (Figure 5).

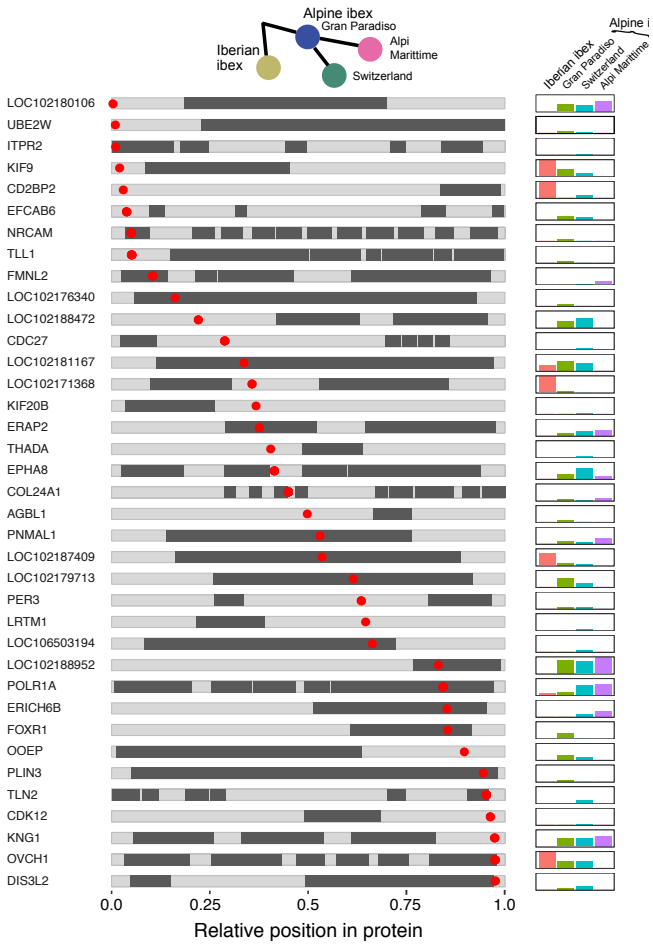

Figure 5: Homology-based inference of the impact of highly deleterious mutations. The localization of protein family (PFAM) domains are highlighted in dark. Red dots indicate the relative position of a highly deleterious mutation segregating in Alpine ibex. The frequencies of highly deleterious mutations are summarized for Iberian ibex and three subsets of Alpine ibex. The demographic history is shown with a schematic.

To ascertain whether accumulation and purging of different mutation classes is indeed expected to occur in the demographic context of the Alpine ibex reintroductions, we parametrized an individual-based forward simulation model with the demographic record[38] (Figure 6A). The model included all populations relevant for the founding of the populations under study and was parametrized with the actual founder size (Figure 6A, S15, Table S1). We used *Rxy* to analyze the evolution of deleterious mutation frequencies through the reintroduction bottlenecks. The simulations showed a deficit of highly deleterious mutations after the reintroduction bottlenecks consistent with purging (Figure 6B). The most bottlenecked Alpi Marittime population also showed evidence of purging of the highly deleterious mutations in the simulated dataset but simultaneously accumulation of mildly deleterious mutations

(Figures 6C, D). Consistent with evidence from *Rxy,* the simulations showed that the number of derived mildly deleterious homozygotes increased with the strength of drift, while no increase was found for highly deleterious mutations (Figure 6D, Figures S17-S20).

Figure 6

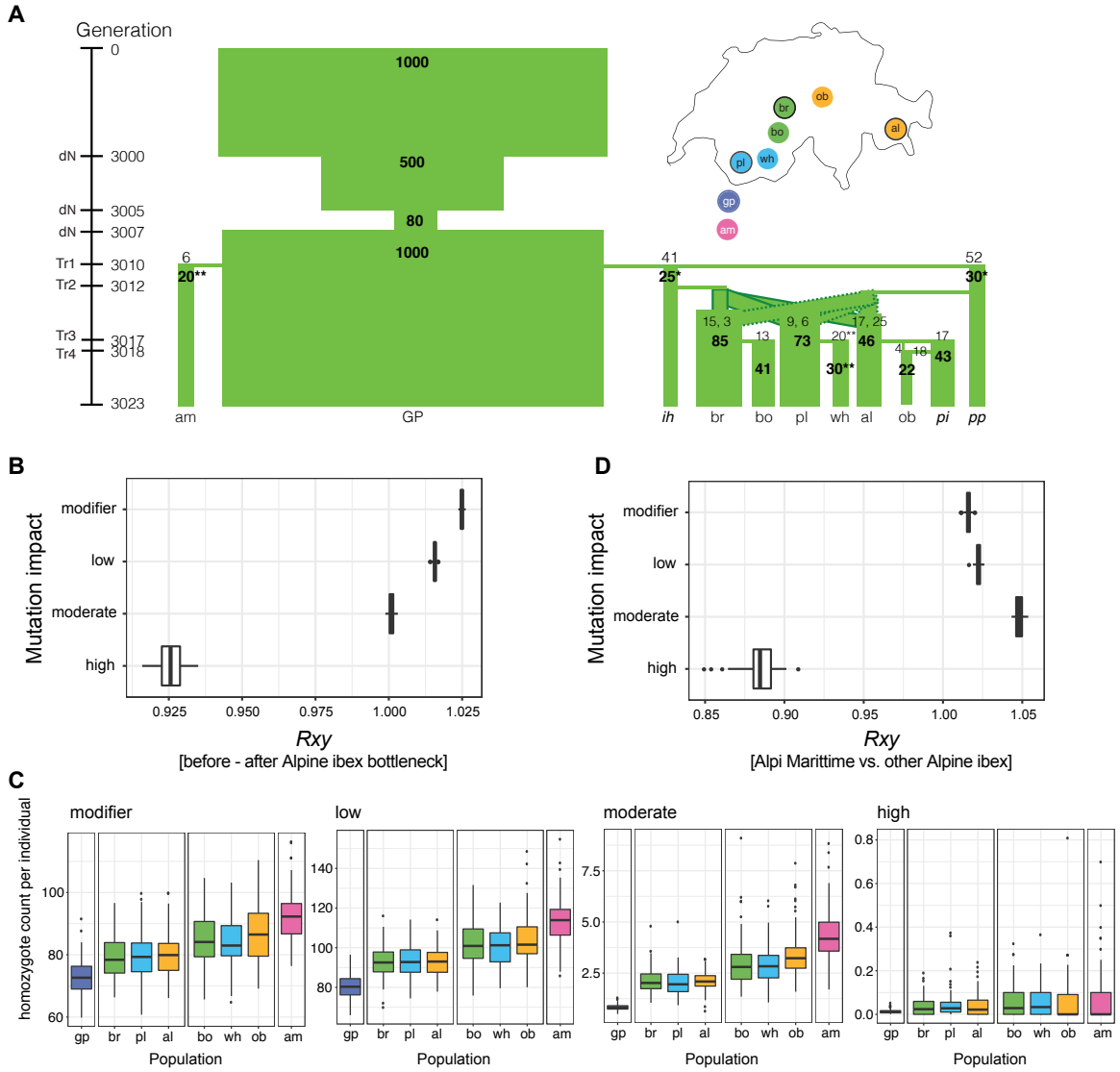

Figure 6: Individual-based forward simulations recapitulating the reintroduction history of Alpine ibex. A) Demographic model used for the individual-based simulations. The model was parametrized using census data and historical records (see methods). Bold numbers represent the carrying capacities defined as the harmonic mean of the census size. Numbers not in bold represent the number of individuals released to found each population. If a population was established from two source populations, the individual numbers are separated by commas. *) Upwards adjusted harmonic means of the census size (historical records were ih=16, Zoo Interlaken Harder, and pp = 20, Wildpark Peter and Paul). The adjustment was necessary to prevent extinction of zoo populations. **) Census numbers were estimated based on historical records of the population but no long- term data census data was available. B) Relative frequency comparison (*Rxy*) of Alpine ibex just before and after the species bottleneck and recolonization. C) *Rxy* analysis contrasting the strongly bottlenecked Alpi Marittime population with all other Alpine ibex populations across the spectrum of impact categories. D) Individual

homozygote counts per impact category. Boxplots summarized 100 population means across simulation replicates. Colors associate founder and descendant populations (see also Figure 3A).

Ibex species with recently reduced population sizes accumulated deleterious mutations compared to closely related species. This accumulation was particularly pronounced in the Iberian ibex that experienced a severe bottleneck and Alpine ibex that went nearly extinct. We show that even though Alpine ibex carry an overall higher mutation burden than related species, the strong bottlenecks imposed by the reintroduction of populations purged highly deleterious mutations, the most bottlenecked population (Alpi Marittime) showing the most purging. However, purging was only effective against the most highly deleterious mutations. Empirical evidence for purging in the wild is scarce [18,19]. Here, we show that a few dozen generations were sufficient to reduce the burden of highly deleterious mutations. This suggests that purging may occur widely in populations undergoing severe bottlenecks. It is important to note that mildly deleterious mutations actually accumulated over the course of the reintroduction, consistent with less efficient selection against mildly deleterious mutations in small populations. Hence, the overall mutation load may have increased with bottleneck strength. This is consistent with the finding that population-level inbreeding, which is a strong indicator of past bottlenecks, is correlated with lower population growth rates in Alpine ibex (Bozzuto et al. *in review*). Our empirical results from the Alpine ibex reintroduction are in line with theoretical predictions that populations with an effective size below 100 individuals can accumulate a substantial burden of mildly deleterious mutations within a relatively short time. The burden of deleterious mutations evident in Iberian ibex supports the notion that even population sizes of ~1000 still accumulate mildly deleterious mutations. High loads of deleterious mutations have been shown to increase the extinction risk of a species [39]. Thus, conservation efforts aimed at keeping effective population sizes above a minimum of 1000 individuals [2] are well justified.

Methods

Genomic data acquisition

DNA samples from 29 Alpine ibex, 4 Iberian ibex, 2 Nubian ibex, 2 Siberian ibex and 1 Markhor individuals were sequenced on an Illumina Hiseq2500 or Hiseq4000 to a depth of 15-38 (median of 17). Table S2 specifies individual sampling locations. Libraries were produced using the TruSeq DNA Nano kit. Illumina sequencing data of 6 Bezoar and 16 domestic goat (coverage 6x – 14x, median 12x) were generated by the NextGen Consortium (https://nextgen.epfl.ch). The corresponding raw data was downloaded from the EBI Short Read Archive: ftp://ftp.sra.ebi.ac.uk/vol1/fastq/.

Read alignment and variant calling

Trimmomatic v.0.36 [40] was used for quality and adapter trimming before reads were mapped to the domestic goat reference genome (version CHIR1, [41]) using Bowtie2 v.2.2.5 [42]. MarkDuplicates from Picard (http://broadinstitute.github.io/picard, v.1.130) was used to mark duplicates. Genotype calling was performed using HaplotypeCaller and GenotypeGVCF (GATK, v.3.6 [43,44]). VariantFiltration of GATK was used to remove single nucleotide polymorphisms (SNP) if: QD <2.0, FS > 40.0, SOR > 5.0, MQ < 20.0, -3.0 > MQRandkSum > 3.0, -3.0 > ReadPosRankSum > 3.0 and AN < 62 (80% of all Alpine ibex individuals). Indels up to 10 bp were also retained and filtered using the same filters and filter parameters, except for not including the filter MQRankSum, because this measure is more likely to be biased for indels of several base pairs. Filtering parameters were chosen based on genome-wide quality statistics distributions (see Figures S21 – S38). Variant positions were independently validated by using the SNP caller Freebayes (v1.0.2-33-gdbb6160 [45]) with the following settings: --no-complex --use-best-n-alleles 6 --min-base-quality 3 --min-mapping-quality 20 --no-population-priors --hwe-priors-off.

To ensure high-quality SNPs, we only retained SNPs that were called and passed filtering using GATK, and that were confirmed by Freebayes. Overall, 97.5 % of all high-quality GATK SNP calls were confirmed by Freebayes. This percentage was slightly lower for chromosome X (96,7%) and unplaced scaffolds (95.2%). We tested whether the independent SNP calls of GATK and Freebayes were concordant and we could validate 99.6% of the biallelic SNPs. We retained genotypes called by GATK.

295 The total number of SNPs detected was 59.5 million among all species. Per species, the number of
296 SNPs ranged from 21.9 million in the domestic goat (N=16) to 2.0 million in Markhor (N=1, Table S2).
297
298 *RNA-seq data generation*
299 Tissue samples of a freshly harvested Alpine ibex female were immediately conserved in RNA*later*
300 (QIAGEN) in the field and stored at -80°C until extraction. The following ten organs were sampled:
301 retina/uvea, skin, heart, lung, lymph, bladder, ovary, kidney, liver and spleen. RNA was extracted using
302 the AllPrep DNA/RNA Mini Kit from Qiagen following the manufacturer's protocol. Homogenization
303 of the samples was performed using a Retsch bead beater (Retsch GmbH) in RLT plus buffer (Qiagen).
304 RNA was enriched using a PolyA enrichment protocol implemented in the TruSeq RNA library
305 preparation kit. Illumina sequencing libraries were produced using the Truseq RNA stranded kit.
306 Sequencing was performed on two lanes of an Illumina Hiseq4000.
307
308 *Genetic diversity and runs of homozygosity*
309 Genetic diversity measured as individual number of heterozygous sites and nucleotide diversity were
310 computed using vcftools [46]. Runs of homozygosity were called using BCFtools/RoH [47], an extension of
311 the software package BCFtools, v.1.3.1. BCFtools/RoH uses a hidden Markov model to detect segments
312 of autozygosity from next generation sequencing data. Due to the lack of a detailed linkage map, we
313 used physical distance as a proxy for recombination rates with the option -M and assuming 1.2cM/Mb
314 following sheep recombination rates [48]. Smaller values for -M led to slightly longer ROH (Figures S3
315 –S5). Because of small per population sample size, we decided to fix the alternative allele frequency
316 (option --AF-dflt) to 0.4. Estimates for the population with the largest sample size (Gran Paradiso, N=7)
317 were very similar if actual population frequencies (option --AF-estimate sp) were used (Figures S4 and
318 S5). Option --viterbi-training was used to estimate transition probabilities before running the HMM.
319 Running the analysis without the option --viterbi-training led to less but longer ROH (Figures S3-S5).
320
321 *Identification of high-confidence deleterious mutations*

322 Three lines of evidence were used to identify high-confidence deleterious mutations. First, variants
323 leading to a functional change are candidates for deleterious mutations. We used snpEff [49] v.4.3 for the
324 functional annotation of each variant. The annotation file ref_CHIR_1.0_top_level.gff3 was
325 downloaded from: ftp://ftp.ncbi.nlm.nih.gov/genomes/Capra_hircus/GFF and then converted to gtf
326 using gffread. Option -V was used to discard any mRNAs with CDS having in-frame stop codons.
327 SnpEff predicts the effects of genetic variants (e.g. stop-gain variants) and assesses the expected impact.
328 The following categories were retrieved: high (e.g. stop-gain or frameshift variant), moderate (e.g
329 missense variant, in-frame deletion), low (e.g. synonymous variant) and modifier (e.g. exon variant,
330 downstream gene variant). In the case of overlapping transcripts for the same variant, we used the
331 primary transcript for further analysis. A total of 49.0 % of all detected SNPs were located in intergenic
332 regions, 43.2 % in introns, 6.5 % down- and upstream of genes. A total of 0.7% of variants were within
333 CDS, of which ~60% were synonymous and ~40% were missense variants. Overall, 0.002 % were stop-
334 gain mutations.
335 Protein sequences were annotated using InterProScan v.5.33 by identifying conserved protein family
336 (PFAM) domains [50].
337
338 Second, we assessed the severity of a variant by its phylogenetic conservation score. A non-
339 synonymous variant is more likely to be deleterious if it occurs in a conserved region of the genome.
340 We used GERP conservation scores, which are calculated as the number of substitutions observed
341 minus the number of substitutions expected from the species tree under a neutral model. We
342 downloaded GERP scores (accessed from http://mendel.stanford.edu/SidowLab), which have been
343 computed for the human reference genome version hg19. The alignment was based on 35 mammal
344 species but did not include the domestic goat (see https://genome.ucsc.edu/cgi-
345 bin/hgTrackUi?db=hg19&g=allHg19RS_BW for more information). Exclusion of the focal species
346 domestic goat is recommended for the computation of conservation scores, as the inclusion of the
347 reference genome may lead to biases [51].

348 In order to remap the GERP scores associated to hg19 positions to the domestic goat reference genome
349 positions, we used liftOver (hgdownload.cse.ucsc.edu, v.287) and the chain file downloaded from
350 hgdownload-test.cse.ucsc.edu/goldenPath/capHir1.
351
352 Third, we ascertained support for gene models annotated in the domestic goat genome with expression
353 analyses of Alpine ibex tissue samples. We included expression data from 10 organs of an Alpine ibex
354 female (see RNA-seq data section above) to assess expression levels of each gene model. Quality
355 filtering of the raw data was performed using Trimmomatic [40] v.0.36. Hisat2 [52] v.2.0.5 was used to map
356 the reads of each organ to the domestic goat reference genome. The mapping was run with option --
357 rna-strandness RF (stranded library) and supported by including a file with known splice sites (option
358 --known-splicesite-infile). The input file was produced using the script hisat2_extract_splice_sites.py
359 (part of hisat2 package) from the same gtf file as the one used for the snpEff analyis (see above). For
360 each organ, featureCounts [53] (subread-1.5.1) was used to count reads per each exon using the following
361 options: -s 2 (reverse stranded) –f (count reads at the exon level), –O (assign reads to all their
362 overlapping features), –C (excluding read pairs mapping to different chromosomes or the same
363 chromosome but on a different strand). The R package edgeR [54] was used to calculate FPKM
364 (Fragments Per Kilobase Of Exon Per Million Fragments Mapped) per each gene and organ. For variant
365 sites that were included in more than one exon, the highest FPKM value was used. We found that 16'013
366 out of 17'998 genes showed transcriptional activity of at least one exon (FPKM > 0.3). Overall 166'973
367 out of 178'504 exons showed evidence for transcription. In a total of 1928 genes, one or more exons
368 showed no evidence for transcription. Retained SNPs were found among 118'756 exons and 17'685
369 genes. Overall 611'711 out of 677'578 SNPs were located in genes with evidence for transcription.
370
371 Deleterious mutations are assumed to be overwhelmingly derived mutations. We used all ibex species
372 except Alpine and Iberian ibex as an outgroup to define the derived state. For each biallelic site, which
373 was observed in alternative state in Alpine ibex or Iberian ibex, the alternative state was defined as
374 derived if its frequency was zero in all other species (a total of 44'730 autosomal SNPs). For loci with
375 more than two alleles, the derived state was defined as unknown. For comparisons among all species,

376 we only used the following criteria to select SNPs (370'853 biallelic SNPs retained): transcriptional
377 activity (FPKM > 0.3 in at least one organ), GERP > -2 and a minimal distance to the next SNP of 3bp.
378
379 *Individual-based simulations with Nemo*
380 Individual-based forward simulations were run using the software Nemo [38] v.2.3.51. A customized
381 version of aNEMOne [55] was used to prepare input files for parameter exploration. The sim.ini file for
382 the final set of parameters run in 100 replicates is available as Supplementary File 1. All populations
383 relevant for the founding of the populations under study were included in the model. See Figure 6A for
384 the simulated demography, which was modeled with the actual founder numbers (assuming a sex-ratio
385 of 1:1), while the translocations were simplified into four phases (data from [37], DRYAD entry
386 doi:10.5061/dryad.274b1 and [36]). The harmonic mean of the population census from the founding up to
387 the final sampling year (2007) was used to define the population carrying capacity. Mating was assumed
388 to be random and fecundity (mean number of offspring per female) set to five. The selection coefficients
389 of 5000 biallelic loci subject to selection were drawn from a gamma distribution with a mean of 0.01
390 and a shape parameter of 0.3 resulting in $s < 1\%$ for 99.2% of all loci [56] (Figure S16). Based on empirical
391 evidence, we assumed a negative relationship between h and s [57]. We used the exponential equation h
392 $= \exp(-51*s)/2$ with a mean h set to 0.37 following [58]. We assumed hard selection acting at the offspring
393 level. In addition to the 5000 loci under selection, we simulated 500 neutral loci. Recombination rates
394 among each neutral or deleterious locus was set to 0.5. This corresponds to an unlinked state. Initial
395 allele frequencies were set to $\mu / h * s = 0.0014$ (corresponding to the expected mean frequency at
396 mutation-selection balance [59]). Mutation rate μ was set to 5e-05 and deleterious mutations were allowed
397 to back-mutate at a rate of 5e-07.

398 A burn-in of 3000 generations was run with one population ($N = 1000$) representing the entire species
399 allowing to reach a quasi-equilibrium. N was reduced to $N = 500$ for five generations before a brief,
400 two generation bottleneck of $N = 80$. At generation 3007, the population recovered to $N = 1000$ and
401 three generations later the reintroduction was started with the founding of the two zoos Interlaken
402 Harder (ih) and Peter and Paul (pp). The founding of new populations was modeled by migration of

offspring into an empty patch.

The zoo ih (Interlaken Harder) and several populations did not survive all replicates of the simulations. Extinction rates were as follows: ih (Zoo Interlaken Harder) 84%, bo (Bire Öschinen) 3%, wh (Weisshorn) 3%, ob (Oberbauenstock) 9%, am (Alpi Marittime) 14% and pil (Pilatus) 2%. The high extinction rate of the zoo Interlaken Harder did not affect the outcome of the simulations. The extinctions were a result of the strong reduction in population size during the founding and occurred always after the founding (see also Figure S15). The extinctions of the reintroduced populations did not affect the estimates of derived allele counts but reduced sample sizes and, hence, affected the variance of estimators.

Data availability

Raw whole-genome sequencing data produced for this project was deposited at the NCBI Short Read Archive under the Accession nos. SAMN10736122–SAMN10736160 (BioProject PRJNA514886). Raw RNA sequencing data produced for this project was deposited at the NCBI Short Read Archive under the Accession nos. SAMN10839218-SAMN10839227 (BioProject PRJNA517635).

Acknowledgments

We thank the following organizations and colleagues who contributed samples to this project. Iris Biebach, the Swiss hunting authorities of the cantons of Bern, Nidwalden, Obwalden, Uri, Graubünden and Wallis; the Gran Paradiso National Park (Alice Brambilla) and the Alpi Marittime National Park (Laura Martinelli), Sebastien Regnaut and Richard Kock, Zoological Society of London, Christian Siegenthaler, Ruedi Kunz and Samer Angelone-Alasaad. We are thankful to Glauco Camenisch and Kasia Sluzek, who provided access to Alpine ibex RNAseq datasets. We thank Laurent Excoffier, Stephan Peischl, Kimberly Gilbert, Heidi Lischer, Stefan Wyder, Thomas Wicker, Alan Brelsford and Jessica Purcell for helpful advice and comments on a previous version of the manuscript. We are grateful for drawings by Nadine Coline of the Zoological Museum of Zürich. This work was supported by the University of Zurich through a University Research Priority Program "Evolution in Action" pilot project grant and the Swiss Federal Office for the Environment. DC and CG were supported by the

Swiss National Science Foundation (grant 31003A_173265 and 31003A_182343, respectively). This study makes use of data generated by the NextGen Consortium, which was supported by grant agreement number 244356 of the European Union's Seventh Framework Programme (FP7/2010-2014).

References:

1. Morton, N. E., Crow, J. F. & Muller, H. J. An estimate of the mutational damage in man from data on consanguineous marriages. *PNAS* **42,** 855–863 (1956).
2. Frankham, R., Bradshaw, C. J. A. & Brook, B. W. Genetics in conservation management: Revised recommendations for the 50/500 rules, Red List criteria and population viability analyses. *Biol Conserv* **170,** 56–63 (2014).
3. Cruz, F., Vilà, C. & Webster, M. T. The legacy of domestication: accumulation of deleterious mutations in the dog genome. *Mol Biol Evol* **25,** 2331–2336 (2008).
4. Renaut, S. & Rieseberg, L. H. The accumulation of deleterious mutations as a consequence of domestication and improvement in sunflowers and other *compositae* crops. *Mol Biol Evol* **32,** 2273–2283 (2015).
5. Lynch, M. Mutation and human exceptionalism: our future genetic load. *Genetics* **202,** 869–875 (2016).
6. Marsden, C. D. *et al.* Bottlenecks and selective sweeps during domestication have increased deleterious genetic variation in dogs. *PNAS* **113,** 152–157 (2016).
7. Laenen, B. *et al.* Demography and mating system shape the genome-wide impact of purifying selection in *Arabis alpina*. *PNAS* **115,** 816–821 (2018).
8. Charlesworth, B. Effective population size and patterns of molecular evolution and variation. *Nat Rev Genet* **10,** 195–205 (2009).
9. Kimura, M. Stochastic processes and distribution of gene frequencies under natural selection. *Cold Spring Harb. Symp. Quant. Biol.* **20,** 33–53 (1955).
10. Keller, L. & Waller, D. Inbreeding effects in wild populations. *Trends Ecol Evol* **17,** 230–241 (2002).
11. Glémin, S. How are deleterious mutations purged? Drift versus nonrandom mating. *Evolution* **57,** 2678–2687 (2003).
12. Garcia-Dorado, A. Understanding and predicting the fitness decline of shrunk populations: inbreeding, purging, mutation, and standard selection. *Genetics* **190,** 1461–1476 (2012).
13. Crow, J. F. Genetic loads and the cost of natural selection. in *Mathematical Topics in Population Genetics* (ed. Kojima, K. I.) 128–177 (Springer-Verlag, 1970).
14. Robinson, J. A. *et al.* Genomic flatlining in the endangered island fox. *Curr Biol* **26,** 1183–1189 (2016).
15. Kirkpatrick, M. & Jarne, P. The effects of a bottleneck on inbreeding depression and the genetic load. *Am Nat* **155,** 154–167 (2000).
16. Bataillon, T. & Kirkpatrick, M. Inbreeding depression due to mildly deleterious mutations in finite populations: size does matter. *Genet Res* **75,** 75–81 (2000).
17. Willi, Y., Fracassetti, M., Zoller, S. & Van Buskirk, J. Accumulation of mutational load at the edges of a species range. *Mol Biol Evol* **22,** 140 (2018).
18. Hedrick, P. W. & Garcia-Dorado, A. Understanding inbreeding depression, purging, and genetic rescue. *Trends Ecol Evol* **31,** 940–952 (2016).
19. Xue, Y. Mountain gorilla genomes reveal the impact of long-term population decline and inbreeding. *Science* **348,** 239–242 (2015).
20. Rogers, R. L. & Slatkin, M. Excess of genomic defects in a woolly mammoth on Wrangel island. *PLoS Genet* **13,** e1006601 (2017).
21. Robinson, J. A., Brown, C., Kim, B. Y., Lohmueller, K. E. & Wayne, R. K. Purging of strongly deleterious mutations explains long-term persistence and absence of inbreeding depression in island foxes. *Curr Biol* 1–13 (2018). doi:10.1016/j.cub.2018.08.066
22. Laws, R. J. & Jamieson, I. G. Is lack of evidence of inbreeding depression in a threatened New Zealand robin indicative of reduced genetic load? *Animal Conservation* **14,** 47–55 (2011).
23. Kennedy, E. S., Grueber, C. E., Duncan, R. P. & Jamieson, I. G. Severe inbreeding depression and no evidence of purging in an extremely inbred wild species--the Chatham Island black robin. *Evolution* **68,** 987–995 (2014).
24. Crnokrak, P. & Barrett, S. Perspective: Purging the genetic load: A review of the experimental evidence. *Evolution* **56,** 2347–2358 (2002).

25. Kalinowski, S. T., Hedrick, P. W. & Miller, P. S. Inbreeding depression in the Speke's gazelle captive breeding program. *Conserv Biol* **14,** 1375–1384 (2000).
26. Grodinsky, C. & Stuwe, M. The reintroduction of the Alpine ibex to the Swiss Alps. *Smithsonian* **18,** 68–77 (1987).
27. Biebach, I. & Keller, L. F. A strong genetic footprint of the re-introduction history of Alpine ibex (*Capra ibex ibex*). *Mol Ecol* **18,** 5046–5058 (2009).
28. Grossen, C., Biebach, I., Angelone-Alasaad, S., Keller, L. F. & Croll, D. Population genomics analyses of European ibex species show lower diversity and higher inbreeding in reintroduced populations. *Evol Appl* **11,** 123–139 (2018).
29. Reading, R. & Shank, C. *Capra sibirica:* The IUCN Red List of Threatened Species 2008. doi:10.2305/IUCN.UK.2008.RLTS.T42398A10695735.en
30. McQuillan, R. *et al.* Runs of homozygosity in European populations. *The American Journal of Human Genetics* **83,** 359–372 (2008).
31. Cooper, G. M. *et al.* Distribution and intensity of constraint in mammalian genomic sequence. *Genome Res* **15,** 901–913 (2005).
32. Couturier, M. *Le Bouquetin des Alpes*. (1962).
33. Do, R. *et al.* No evidence that selection has been less effective at removing deleterious mutations in Europeans than in Africans. *Nature* **47,** 126–131 (2015).
34. Terrier, G. & Rossi, P. Le bouquetin (*Capra ibex ibex*) dans les alpes maritimes franco-italiennes: occupation de l'éspace, clonisation et régulation naturelles. *Traveaux Scientifiques du Parc National de la Vanoise* **XVIII,** 271–288 (1994).
35. Maudet, C. *et al.* Microsatellite DNA and recent statistical methods in wildlife conservation management: applications in Alpine ibex *Capra ibex (ibex)*. *Mol Ecol* **11,** 421–436 (2002).
36. Biebach, I. & Keller, L. F. Inbreeding in reintroduced populations: the effects of early reintroduction history and contemporary processes. *Conserv Genet* **11,** 527–538 (2010).
37. Aeschbacher, S., Futschik, A. & Beaumont, M. A. Approximate Bayesian computation for modular inference problems with many parameters: the example of migration rates. *Mol Ecol* **22,** 987–1002 (2013).
38. Guillaume, F. & Rougemont, J. Nemo: an evolutionary and population genetics programming framework. *Bioinformatics* **22,** 2556–2557 (2006).
39. Lynch, M., Conery, J. & Burger, R. Mutation accumulation and the extinction of small populations. *Am Nat* **146,** 489–518 (1995).
40. Bolger, A. M., Lohse, M. & Usadel, B. Trimmomatic: a flexible trimmer for Illumina sequence data. *Bioinformatics* **30,** 2114–2120 (2014).
41. Dong, Y. *et al.* Sequencing and automated whole-genome optical mapping of the genome of a domestic goat (*Capra hircus*). *Nat Biotechnol* **31,** 135–141 (2012).
42. Langmead, B. & Salzberg, S. L. Fast gapped-read alignment with Bowtie 2. *Nature Methods* **9,** 357–359 (2012).
43. McKenna, A. *et al.* The Genome Analysis Toolkit: a MapReduce framework for analyzing next-generation DNA sequencing data. *Genome Res* **20,** 1297–1303 (2010).
44. DePristo, M. A. *et al.* A framework for variation discovery and genotyping using next-generation DNA sequencing data. *Nat Genet* **43,** 491–498 (2011).
45. Garrison, E. FreeBayes source repository. Available at: https://github.com/ekg/freebayes. (Accessed: 14 November 2018)
46. Danecek, P. *et al.* The variant call format and VCFtools. *Bioinformatics* **27,** 2156–2158 (2011).
47. Narasimhan, V. *et al.* BCFtools/RoH: a hidden Markov model approach for detecting autozygosity from next-generation sequencing data. *Bioinformatics* **32,** 1749–1751 (2016).
48. Dumont, B. L.Payseur, Bret A. Evolution of the genomic rate of recombination in mammals. *Evolution* **62,** 276–294 (2008).
49. Cingolani, P. *et al.* A program for annotating and predicting the effects of single nucleotide polymorphisms, SnpEff: SNPs in the genome of Drosophila melanogaster strain w(1118); iso-2; iso-3. *fly* **6,** 80–92 (2012).
50. Jones, P. *et al.* InterProScan 5: genome-scale protein function classification. *Bioinformatics* **30,** 1236–1240 (2014).

51. Fu, W., Gittelman, R. M., Bamshad, M. J. & Akey, J. M. Characteristics of neutral and deleterious protein-coding variationamong individuals and populations. *Am J Hum Genet* **95,** 421–436 (2014).
52. Kim, D., Langmead, B. & Salzberg, S. L. HISAT: a fast spliced aligner with low memory requirements. *Nature Methods* **12,** 357–360 (2015).
53. Liao, Y., Smyth, G. K. & Shi, W. featureCounts: an efficient general purpose program for assigning sequence reads to genomic features. *Bioinformatics* **30,** 923–930 (2014).
54. Robinson, M. D., McCarthy, D. J., Bioinformatics, G. S.2010. edgeR: a Bioconductor package for differential expression analysis of digital gene expression data. *academic.oup.com*
55. kjgilbert/aNEMOne. (2017).
56. Keightley, P. D. The distribution of mutation effects on viability in Drosophila melanogaster. *Genetics* **138,** 1315–1322 (1994).
57. Agrawal, A. F. & Whitlock, M. C. Inferences about the distribution of dominance drawn from yeast gene knockout data. *Genetics* **187,** 553–566 (2011).
58. Gilbert, K. J. *et al.* Local Adaptation Interacts with Expansion Load during Range Expansion: Maladaptation Reduces Expansion Load. *Am Nat* **189,** 368–380 (2017).
59. Crow, J. F. & Kimura, M. *An Introduction to Population Genetics Theory*. (New Jersey: Blackburn Press, 1970).
60. IUCN 2018. *httpwww.iucnredlist.org* Available at: (Accessed: 10 November 2018)

Figure legends

Figure 1: Characterization of sampled ibex species. A) Geographical distribution and IUCN conservation status of ibex and wild goat species (LC: Least concern, V: Vulnerable, NT: Near threatened [60]). Sample sizes: *C. ibex*: N=29, *C. pyrenaica*: N=4, *C. aegagrus*: N=6, *C. sibirica*: N=2, *C. falconeri*: N=1, *C. nubiana*: N=2. B) Maximum likelihood phylogenetic analyses, C) nucleotide diversity, D) proportion of the genome with runs of homozygosity (ROH) longer than 2.5 Mb and E) percentage of polymorphic sites within species that segregate highly deleterious mutations.

Figure 2: Segregating deleterious mutations in Alpine and Iberian ibex. A) Population sampling locations of Iberian ibex (left, grey circles) and Alpine ibex (right, colored circles). Each filled circle represents a population. Circles with a black outline indicate the first three reintroduced populations in Switzerland that were used for all subsequent population reintroductions of Alpine ibex. Colors associate founder and descendant populations (see also Figure 3A). Site frequency spectra for neutral (modifier), mildly (moderate impact) and highly deleterious (high impact) mutations for (B) Iberian

582 and (C) Alpine ibex. D) *Rxy* analysis contrasting Iberian with Alpine ibex across the spectrum of impact
583 categories. *Rxy* < 1 indicates a relative frequency deficit of the corresponding category in Alpine ibex
584 compared to Iberian ibex. E) Individual homozygote counts per impact category for Iberian (light green)
585 and Alpine ibex (dark green).
586
587 **Figure 3: Population genomic consequences of Alpine ibex recolonization**. A) Schematic showing
588 the recolonization history and population pedigree of Alpine ibex. Locations include also zoos and the
589 population Pilatus (pi), which was not sampled for this study but is known to have contributed to the
590 population Oberbauenstock (ob). am: Alpi Marittime, gp: Gran Paradiso; ih: Zoo Interlaken Harder; al:
591 Albris; bo: Bire Öschinen; br: Brienzer Rothorn; ob: Oberbauenstock; pl: Pleureur; rh: Rheinwald; wh:
592 Weisshorn; pi: Pilatus; pp: Wildpark Peter and Paul. The grey circle represents a population that was
593 founded from more than one population. Figure elements were modified from Biebach and Keller
594 (2009) with permission. B) Principal component analysis of all Alpine ibex individuals included in the
595 study. C) Nucleotide diversity per population. D) Proportion of the genome within runs of
596 homozygosity (ROH) longer than 2.5 Mb. E) *Rxy* analysis contrasting the strongly bottlenecked Alpi
597 Marittime population with all other Alpine ibex populations across the spectrum of impact categories.
598 *Rxy* < 1 indicates a relative frequency deficit of the corresponding category in the Alpi Marittime
599 population. Circles with a black outline indicate the first three reintroduced populations in Switzerland
600 that were used for all subsequent population reintroductions of Alpine ibex. Colors associate founder
601 and descendant populations.
602
603 **Figure 4: Impact of recolonization on the mutation load per individual.** (A) Homozygote counts
604 and (B) allele counts per individual for each Alpine ibex population. The schematic between A and B
605 indicates the harmonic mean of the census size of each population, which is inversely correlated with
606 the strength of drift. *) Estimated numbers. Colors associate founder and descendant populations (see
607 also Figure 3A).
608

609 **Figure 5: Homology-based inference of the impact of highly deleterious mutations.** The
610 localization of protein family (PFAM) domains are highlighted in dark. Red dots indicate the relative
611 position of a highly deleterious mutation segregating in Alpine ibex. The frequencies of highly
612 deleterious mutations are summarized for Iberian ibex and three subsets of Alpine ibex. The
613 demographic history is shown with a schematic.
614
615 **Figure 6: Individual-based forward simulations recapitulating the reintroduction history of**
616 **Alpine ibex**. A) Demographic model used for the individual-based simulations. The model was
617 parametrized using census data and historical records (see methods). Bold numbers represent the
618 carrying capacities defined as the harmonic mean of the census size. Numbers not in bold represent
619 the number of individuals released to found each population. If a population was established from two
620 source populations, the individual numbers are separated by commas. *) Upwards adjusted harmonic
621 means of the census size (historical records were ih = 16 and pp = 20). The adjustment was necessary
622 to prevent extinction of zoo populations. **) Census numbers were estimated based on historical
623 records of the population but no long- term data census data was available. B) Relative frequency
624 comparison (*Rxy*) of Alpine ibex just before and after the species bottleneck and recolonization. C)
625 *Rxy* analysis contrasting the strongly bottlenecked Alpi Marittime population with all other Alpine
626 ibex populations across the spectrum of impact categories. D) Individual homozygote counts per
627 impact category. Boxplots summarized 100 population means across simulation replicates. Colors
628 associate founder and descendant populations (see also Figure 3A).

Figure 1

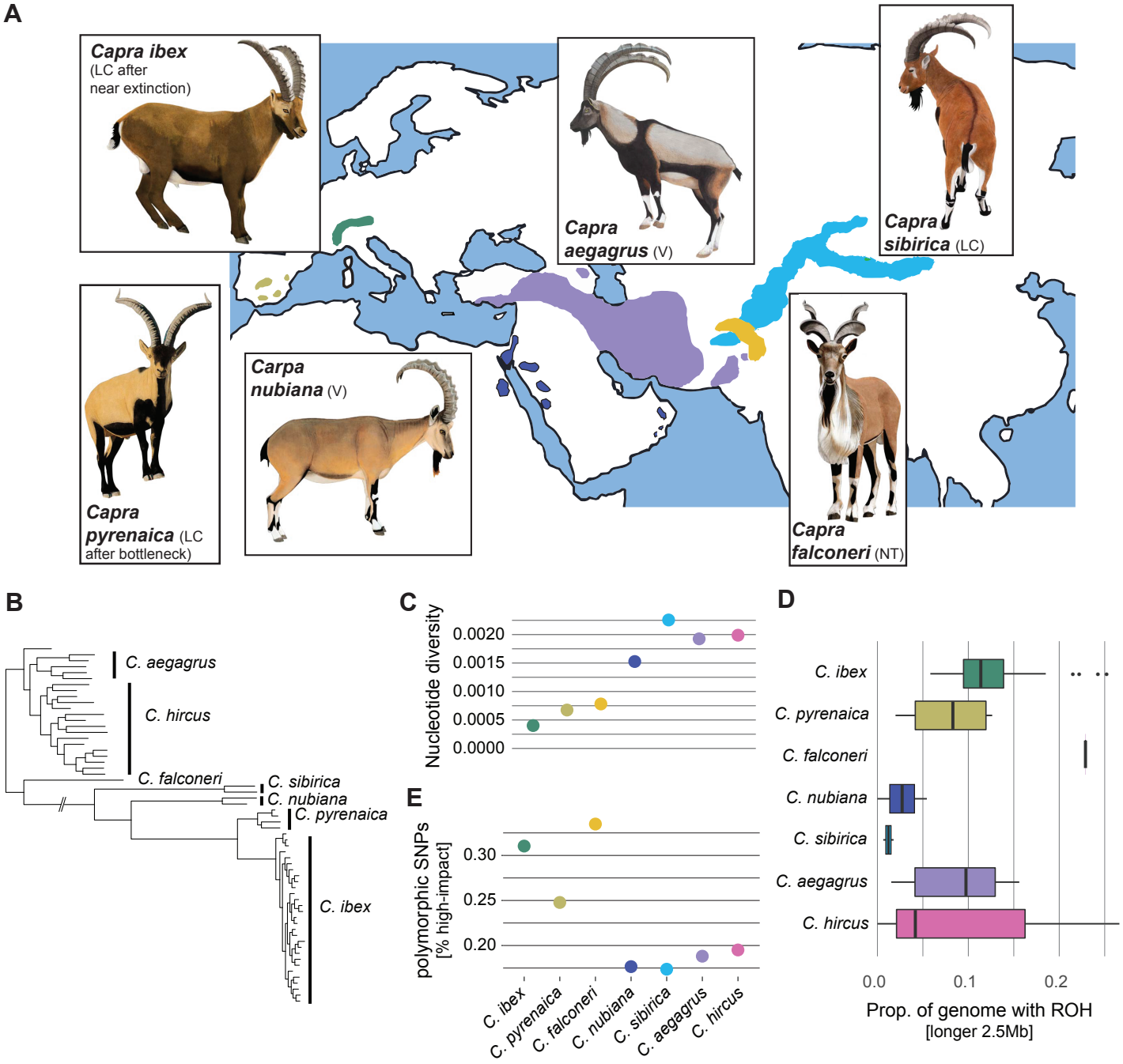
A
Capra ibex
(LC after
near extinction)
Capra
aegagrus (V)
Capra
sibirica (LC)
Capra
pyrenaica (LC
after bottleneck)
Carpa
nubiana (V)
Capra
falconeri (NT)
B
C. aegagrus
C. hircus
C. falconeri
C. sibirica
C. nubiana
C. pyrenaica
C. ibex
C
Nucleotide diversity
0.0020
0.0015
0.0010
0.0005
0.0000
E
polymorphic SNPs
[% high-impact]
0.30
0.25
0.20
C. ibex
C. pyrenaica
C. falconeri
C. nubiana
C. sibirica
C. aegagrus
C. hircus
D
C. ibex
C. pyrenaica
C. falconeri
C. nubiana
C. sibirica
C. aegagrus
C. hircus
0.0
0.1
0.2
Prop. of genome with ROH
[longer 2.5Mb]

Figure 2

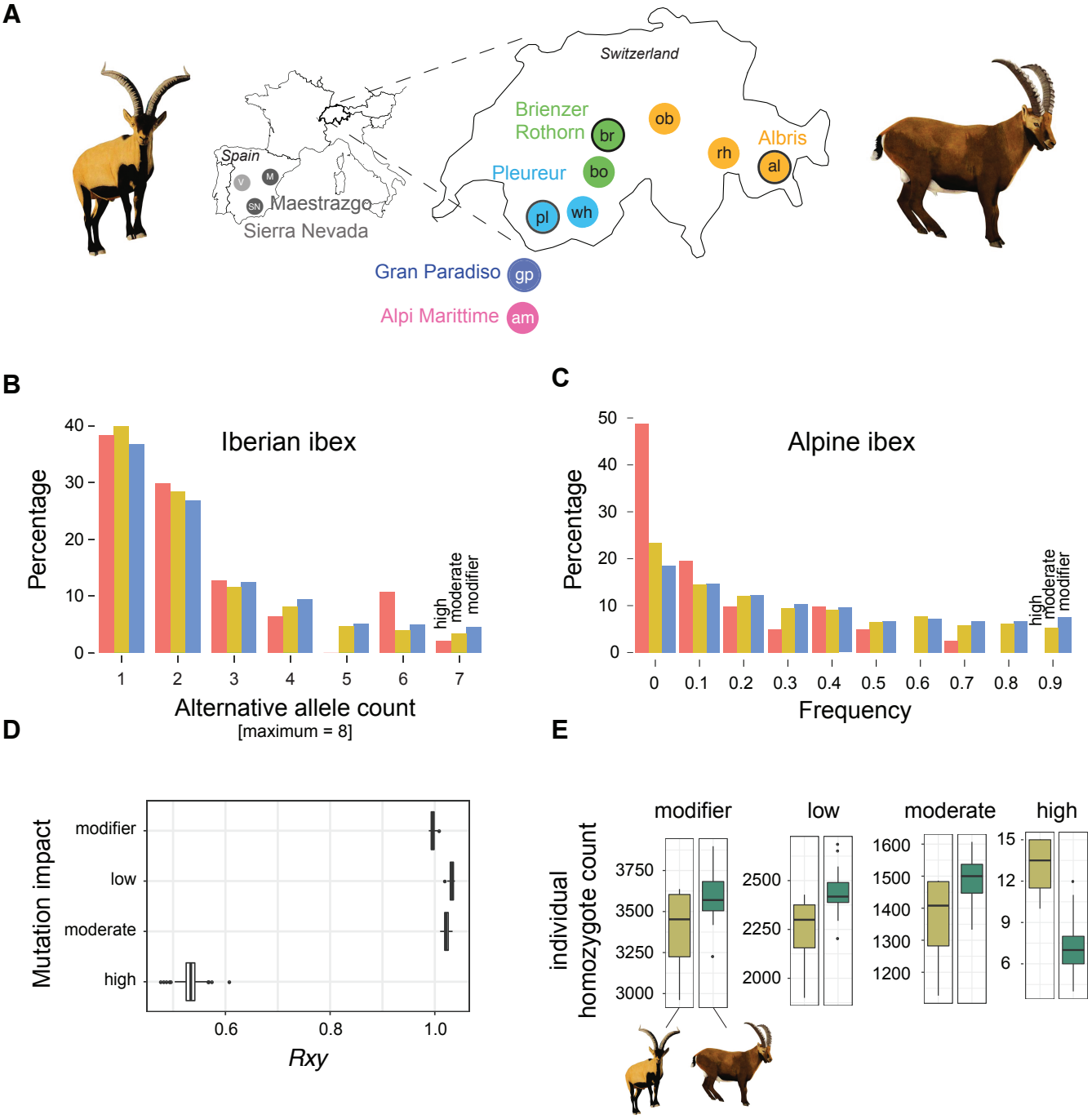
A
Switzerland
Spain
Maestrazgo
Sierra Nevada
Brienzer Rothorn
br
ob
rh
Albris
al
Pleureur
bo
pl
wh
Gran Paradiso
gp
Alpi Marittime
am
B
Iberian ibex
Percentage
Alternative allele count
[maximum = 8]
high
moderate
modifier
C
Alpine ibex
Percentage
Frequency
D
Mutation impact
modifier
low
moderate
high
Rxy
E
modifier
low
moderate
high
individual homozygote count

Figure 3

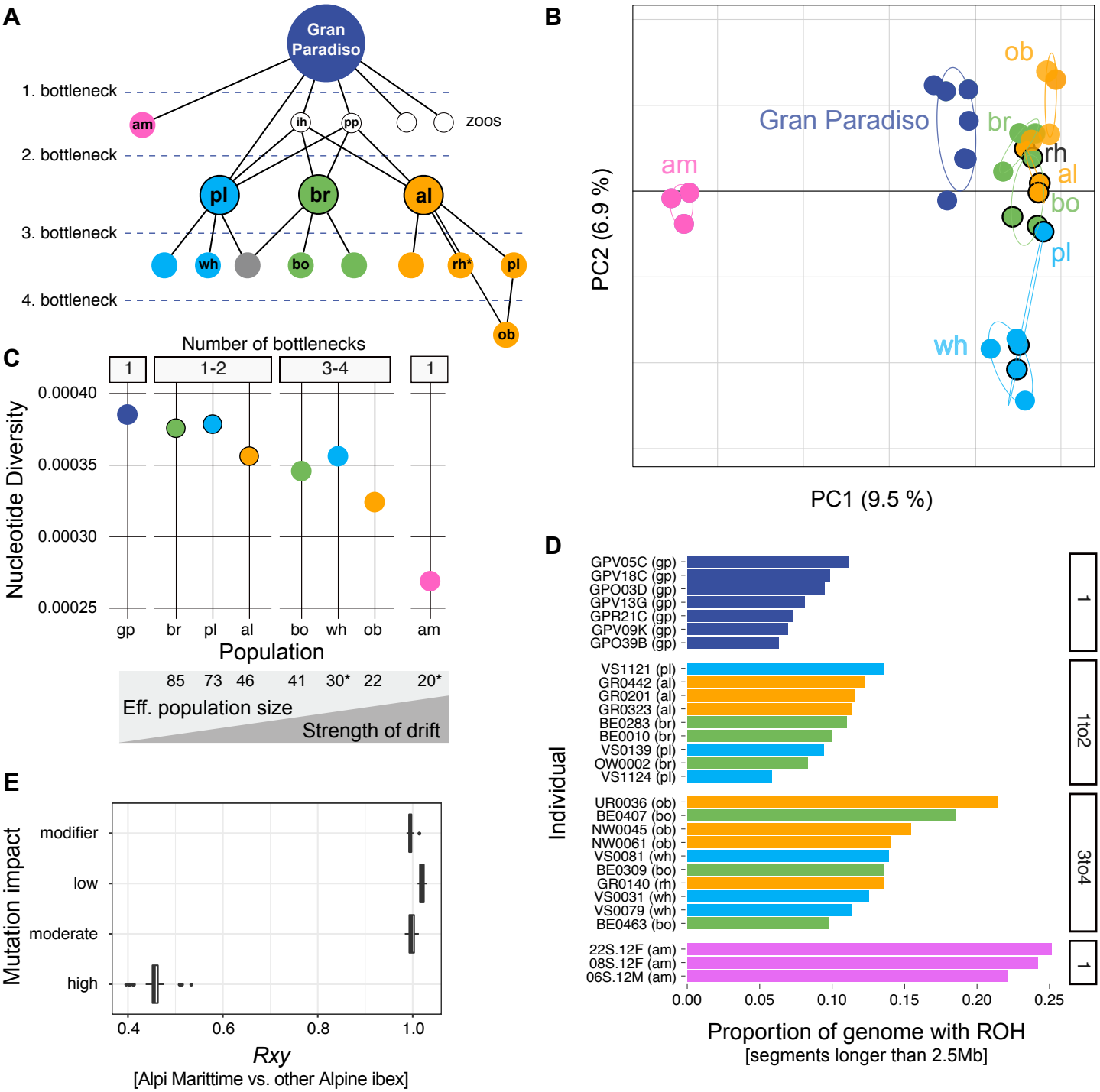
A
Gran Paradiso
1. bottleneck
2. bottleneck
3. bottleneck
4. bottleneck
am
ih
pp
zoos
pl
br
al
wh
bo
rh*
pi
ob
B
Gran Paradiso
ob
br
rh
al
bo
pl
am
wh
PC2 (6.9 %)
PC1 (9.5 %)
C
Number of bottlenecks
1
1-2
3-4
1
Nucleotide Diversity
0.00040
0.00035
0.00030
0.00025
gp
br
pl
al
bo
wh
ob
am
Population
85
73
46
41
30*
22
20*
Eff. population size
Strength of drift
D
Individual
GPV05C (gp)
GPV18C (gp)
GPO03D (gp)
GPV13G (gp)
GPR21C (gp)
GPV09K (gp)
GPO39B (gp)
VS1121 (pl)
GR0442 (al)
GR0201 (al)
GR0323 (al)
BE0283 (br)
BE0010 (br)
VS0139 (pl)
OW0002 (br)
VS1124 (pl)
UR0036 (ob)
BE0407 (bo)
NW0045 (ob)
NW0061 (ob)
VS0081 (wh)
BE0309 (bo)
GR0140 (rh)
VS0031 (wh)
VS0079 (wh)
BE0463 (bo)
22S.12F (am)
08S.12F (am)
06S.12M (am)
1
1to2
3to4
1
0.00
0.05
0.10
0.15
0.20
0.25
Proportion of genome with ROH
[segments longer than 2.5Mb]
E
Mutation impact
modifier
low
moderate
high
0.4
0.6
0.8
1.0
Rxy
[Alpi Marittime vs. other Alpine ibex]

Figure 4

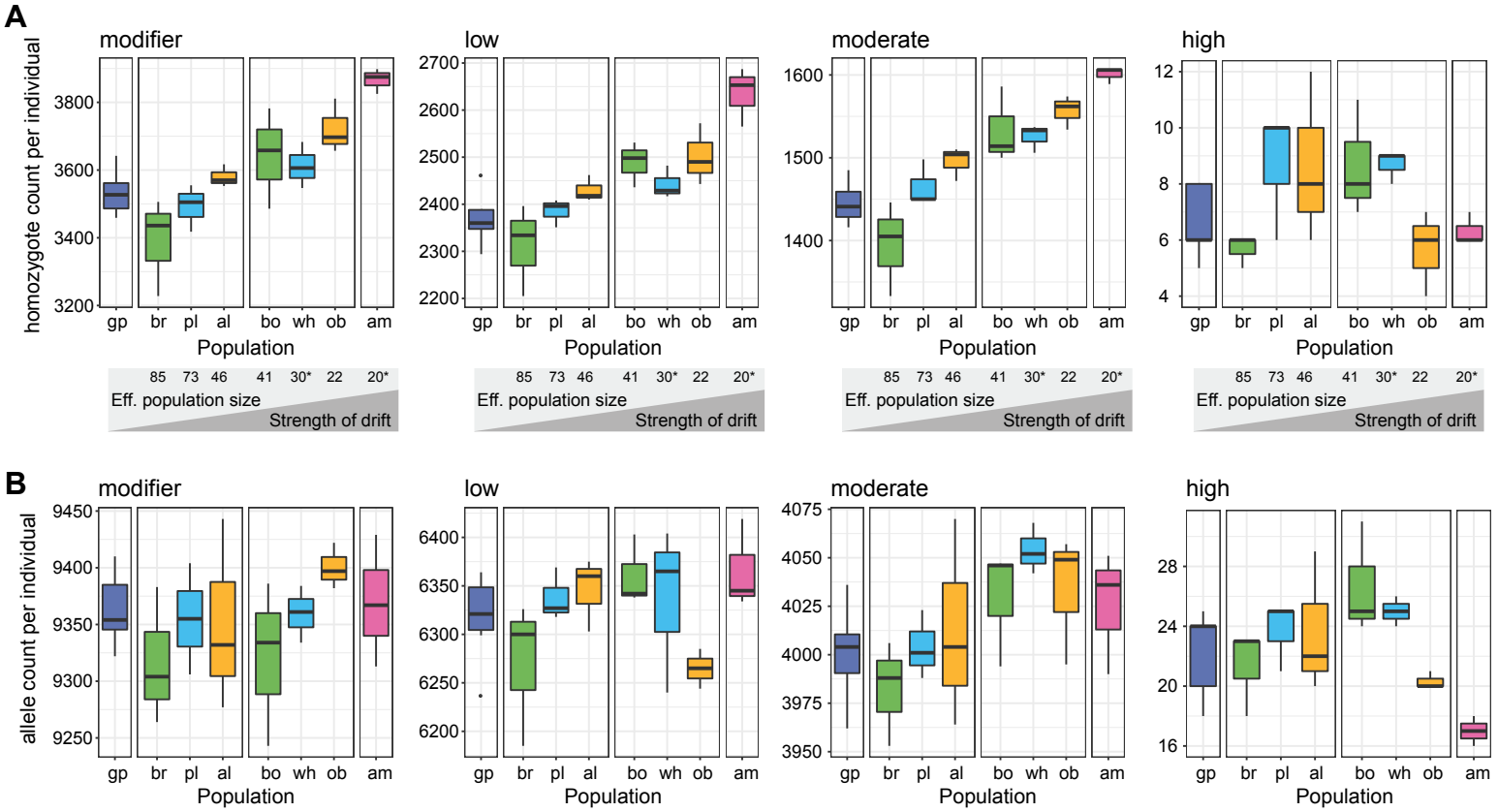
A
modifier
low
moderate
high
homozygote count per individual
gp br pl al bo wh ob am
Population
85 73 46 41 30* 22 20*
Eff. population size
Strength of drift
B
allele count per individual

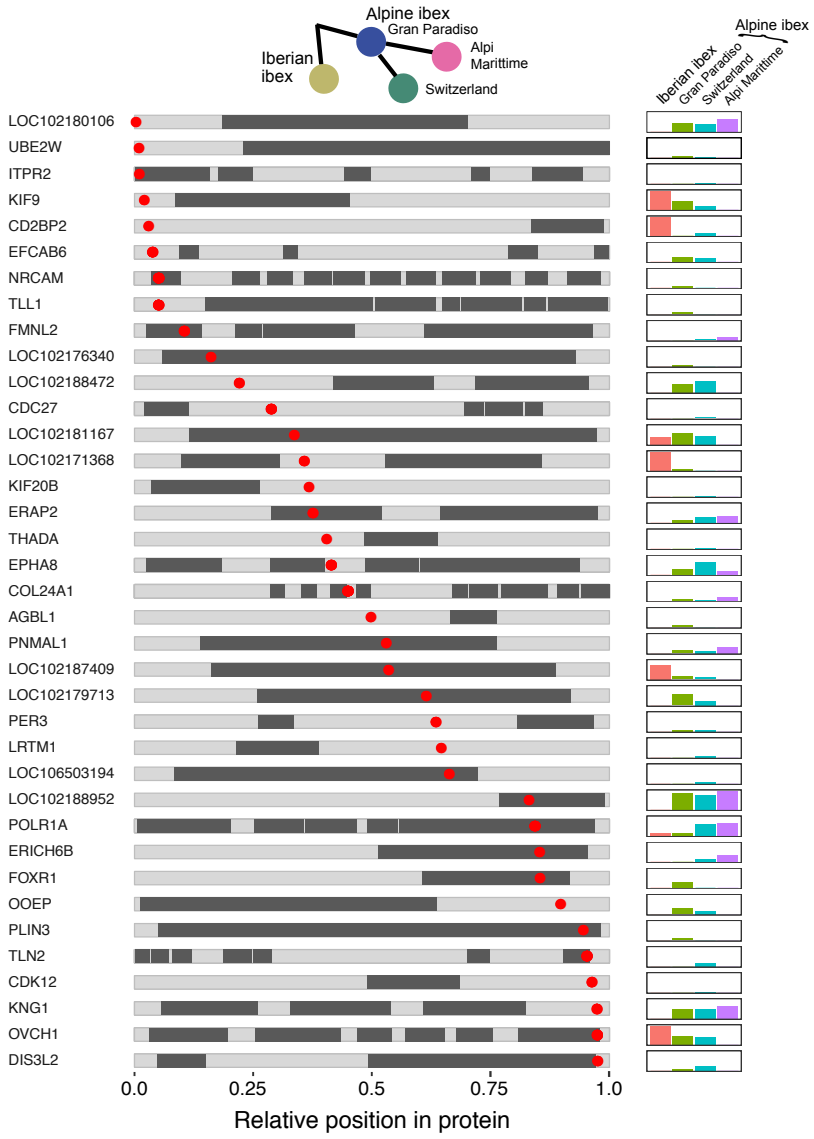
Alpine ibex
Gran Paradiso
Iberian ibex
Alpi Marittime
Switzerland
Alpine ibex
Iberian ibex
Gran Paradiso
Switzerland
Alpi Marittime
LOC102180106
UBE2W
ITPR2
KIF9
CD2BP2
EFCAB6
NRCAM
TLL1
FMNL2
LOC102176340
LOC102188472
CDC27
LOC102181167
LOC102171368
KIF20B
ERAP2
THADA
EPHA8
COL24A1
AGBL1
PNMAL1
LOC102187409
LOC102179713
PER3
LRTM1
LOC106503194
LOC102188952
POLR1A
ERICH6B
FOXR1
OOEP
PLIN3
TLN2
CDK12
KNG1
OVCH1
DIS3L2
0.0
0.25
0.5
0.75
1.0
Relative position in protein

Figure 6

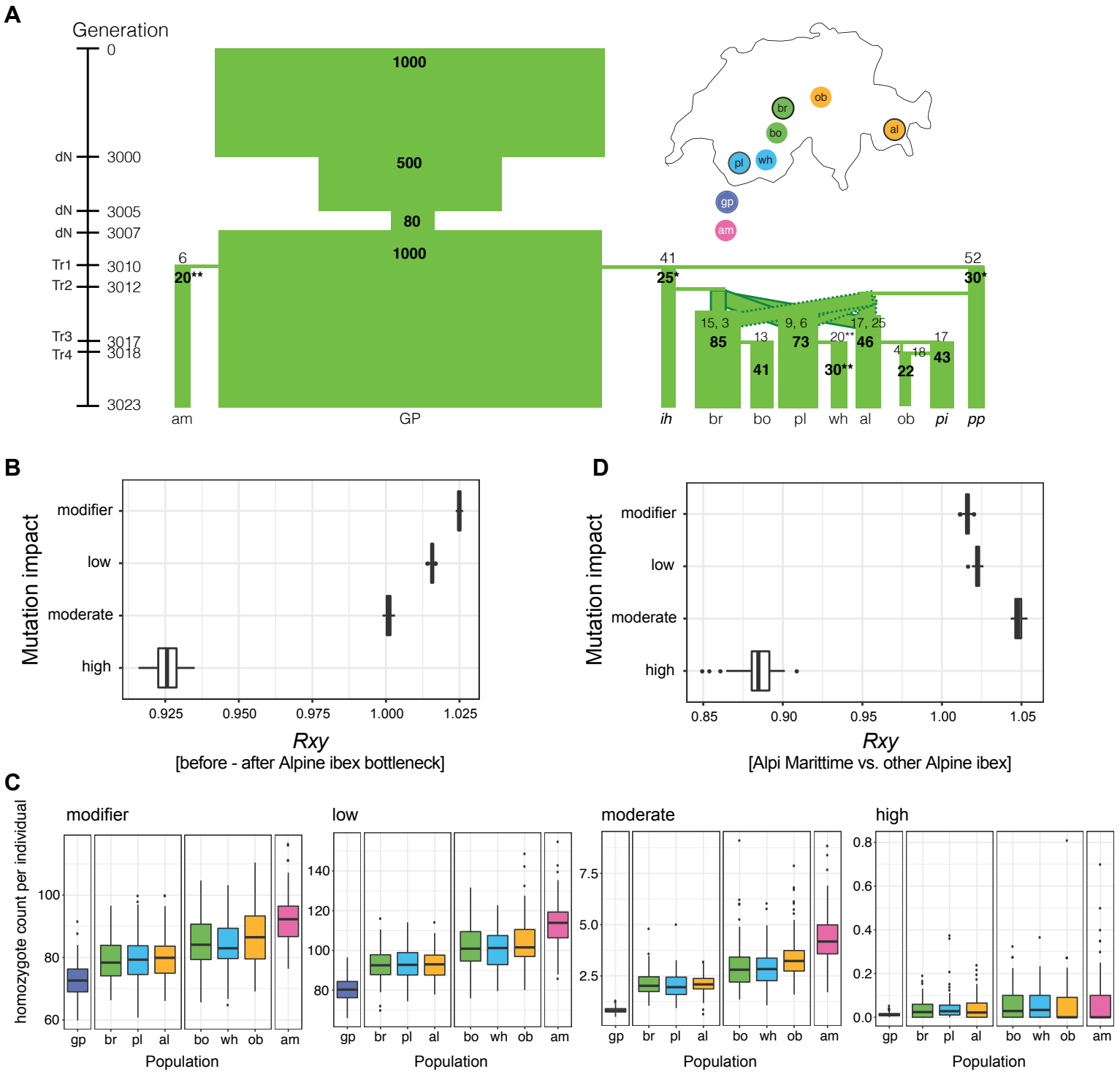
A
Generation
0
dN 3000
dN 3005
dN 3007
Tr1 3010
Tr2 3012
Tr3 3017
Tr4 3018
3023
1000
500
80
1000
6
20**
41
25*
52
30*
15, 3
85
13
41
9, 6
73
20**
30**
17, 25
46
4
18
22
17
43
am
GP
ih
br
bo
pl
wh
al
ob
pi
pp
ob
br
bo
al
pl
wh
gp
am
B
Mutation impact
modifier
low
moderate
high
0.925
0.950
0.975
1.000
1.025
Rxy
[before - after Alpine ibex bottleneck]
D
Mutation impact
modifier
low
moderate
high
0.85
0.90
0.95
1.00
1.05
Rxy
[Alpi Marittime vs. other Alpine ibex]
C
homozygote count per individual
modifier
low
moderate
high
gp br pl al bo wh ob am
Population